The use of variable temperature ^{13}C solid-state MAS NMR and GIPAW DFT calculations to explore the dynamics of diethylcarbamazine citrate

Tiago Venâncio [a,e,], Lyege Magalhaes Oliveira [a], Tomasz Pawlak [b,e], Javier Ellena [c], Nubia Boechat [d], Steven P. Brown [e]*

[a] *Departamento de Química, Universidade Federal de São Carlos, Rodovia Washington Luis, km 235, São Carlos, SP, 13565-905, Brazil.*

[b] *Polish Academy of Sciences, Centre of Molecular and Macromolecular Studies, Sienkiewicza 112, PL-90-363 Łodz, Poland.*

[c] *Instituto de Física de São Carlos, Universidade de São Paulo, Av. Trabalhador são-carlense, 400, São Carlos, SP, 13566-590, Brazil.*

[d] *Fundação Oswaldo Cruz - FioCruz, Instituto de Tecnologia em Fármacos-FarManguinhos, Rua Sizenando Nabuco 100, Rio de Janeiro, RJ, 21041-250, Brazil.*

[e] *Department of Physics, University of Warwick, Coventry, CV4 7AL, UK*

Abstract

Experimental ^{13}C solid-state magic-angle spinning (MAS) NMR as well as DFT (gauge-including projector augmented wave) GIPAW calculations were used to probe disorder and local mobility in diethylcarbamazine citrate, $(DEC)^+(citrate)^-$. This compound has been used as the first option drug for the treatment of filariasis, a disease endemic in tropical countries and caused by adult worms of *Wuchereria bancrofti*, which is transmitted by mosquitoes. We firstly present 2D ^{13}C-^{1}H dipolar-coupling mediated heteronuclear correlation spectra recorded at moderate spinning frequency, to explore the intermolecular interaction between DEC and citrate molecules. Secondly, we investigate the dynamic behaviour of $(DEC)^+(citrate)^-$ by varying the temperature and correlating the experimental MAS NMR results with DFT GIPAW calculations that consider two $(DEC)^+$ conformers (in a 70:30 ratio) for crystal structures determined at 293 and 235 K. Solid-state NMR provides insights on slow exchange dynamics revealing conformational changes involving particularly the diethylcarbamazine ethyl groups.

Keywords: NMR crystallography, diethylcarbamazine citrate, DFT GIPAW calculations, dynamics, chemical shifts

Introduction

Molecular mobility in organic and inorganic solids is important because it can predict changes in the crystal structure [1-5]. In the solid state, intra- and intermolecular interactions have an important effect on the observed molecular mobility and consequently the stability of the crystal structure [6]. In some cases, these local dynamics are responsible for phase transitions between two or more metastable forms and (un)desired polymorphs can be obtained [2, 4, 7-11]. Therefore, the characterization of these processes is important and can be achieved by X-ray diffraction (XRD) methods as well as solid-state NMR [12-17]. For organic compounds, such as active pharmaceutical ingredients, XRD methods can be used to describe some molecular disorder with good precision, but a description of local dynamics remains challenging [18]. For these cases, solid-state NMR is an invaluable technique, due to its high sensitivity to small changes in the orientation of specific chemical moieties, as revealed, for example, by changes in their chemical shifts [19].

This paper applies solid-state NMR to probe disorder and local mobility in diethylcarbamazine dihydrogen citrate, referred to here as diethylcarbamazine citrate, $(DEC)^{+}(citrate)^{-}$ or simply DEC-cit. This compound has been used as the first option drug for the treatment of filariasis, a disease endemic in tropical countries and caused by adult worms of *Wuchereria bancrofti,* which is transmitted by mosquitoes [20, 21]. Due to its good thermal stability, DEC-cit can be added to the table salt used by patients, to guarantee a good adherence to the treatment [20, 22, 23]. Silva and co-workers [24] described the existence of three different phase transitions, leading to four different crystal packings at 293, 235, 150 and 100 K. Additionally, they also reported the existence of two possible conformers (in a 70:30 ratio) for the 293 and 235 K crystal structures due to the existence of a disorder in one of the two ethyl branches of the diethylcarbamazine unit. In a separate paper, we have presented ^{1}H fast magic-angle spinning (MAS) NMR spectra for DEC-cit as well as a GIPAW (gauge-including projector augmented wave) calculation of NMR parameters for the 70% conformer of the 293 K structure [25]. In this paper, we examine the temperature dependence of the ^{13}C chemical shifts and present GIPAW calculations for all the distinct crystal structures and conformers reported by Silva et al. In particular, we observe dynamics for the dihydrogen citrate molecule, for which there is little discussion of disorder in Ref. [24].

The use of solid-state NMR for studying dynamic processes in solid samples is not new, but the challenge resides in the complexity of the molecular packing in crystalline structures such

as biomolecules, as well as for flexible domains in small molecules [19, 26]. Among several NMR parameters used to study dynamics are changes in the chemical shifts and linewidth, as well as also changes in relaxation times and the magnitude of anisotropic interactions (dipolar coupling, chemical shift anisotropy, quadrupolar interaction) [18, 19, 26-29]. In this context, the use of an NMR crystallography approach that combines experimental high resolution solid-state NMR with GIPAW calculations is a promising strategy [19, 30]. This combination permits an investigation of which atoms are involved in the dynamics, since their chemical shifts change according to their new orientations. Hence, our strategy was to use the DEC-cit crystal structures previously determined by XRD at different temperatures and use the NMR crystallography approach to evaluate the dynamics of DEC-cit based on the chemical shift variations. For this purpose, we used DFT GIPAW calculations to obtain the chemical shifts of six different structures at room and low temperatures together with ^{13}C experimental solid-state NMR for evaluating the dynamics over the temperature range from –40 and +50 ºC. Specifically, we firstly describe the use of 2D ^{13}C-^{1}H heteronuclear correlation modulated by dipolar couplings at moderate spinning frequency, to explore the intermolecular interaction between DEC and citrate molecules. Secondly, we describe the dynamic behaviour of DEC-cit by varying the temperature and correlating the experimental MAS NMR results with DFT GIPAW calculations. We were able to explore the disorder of the ethyl moieties in DEC as well as the phase transition between two phases of DEC-cit, focusing on the citrate molecule.

Experimental and computational details

Experimental

Sample and packing: the active pharmaceutical ingredient, diethylcarbamazine citrate, was kindly donated by Fundação Oswaldo Cruz – Farmanguinhos, Rio de Janeiro, and used as received. Approximately 60 mg of the powdered sample were packed into a 4 mm zirconia MAS NMR rotor.

^{13}C detected MAS NMR experiments: ^{1}H-^{13}C cross polarization (CP) MAS experiments were performed using a Bruker Avance III spectrometer operating with a narrow bore 11.7 T magnet (500 MHz for ^{1}H resonance frequency) and equipped with a HXY probehead for 4 mm rotors. A MAS frequency of 5 kHz was used. A two pulse phase modulated TPPM-15 scheme [31, 32] was used for ^{1}H decoupling at a nutation frequency of 83.3 kHz. CP was

applied by using a 90-100% amplitude ramp on ^{1}H [33] during a contact time of 2 ms. 256 transients were coadded with a recycle delay of 3 s. Adamantane was used as an external reference for tetramethylsilane (TMS), setting the CH_2 signal to 38.5 ppm [34, 35].

2D CP - ^{1}H (FSLG)-^{13}C Heteronuclear Correlation [36]: two different experiments (by varying contact time) were performed using a Bruker Avance III spectrometer operating with a wide bore 11.7 T magnet (500 MHz for ^{1}H resonance frequency) and using a 4 mm HXY probehead at a MAS frequencies of 12.5 kHz (for short contact time experiment) and 10.0 kHz (for long contact time experiment), at 22 ^{o}C. Both homonuclear (FSLG, [37, 38]) and heteronuclear SPINAL-64 [39] ^{1}H decoupling employed a nutation frequency of 100 kHz. For each of 128 t_1 FIDs (using the States method to achieve sign discrimination in F_1 with a rotor asynchronized increment of 36 μs for LG period). For short contact time experiment 16 transients were coadded with a recycle delay of 11 s, corresponding to a total experimental time of 6.5 h. For long contact time experiment 64 transients were coadded with a recycle delay of 2.5 s, corresponding to a total experimental time of 3 h. For CP (contact time of 50 and 2000 μs), a 90-100% amplitude ramp on ^{1}H was employed [33]. The scaling factor in F_1 was 0.56 (50 μs) and 0.55 (2000 μs). ^{13}C chemical shifts were referenced using *L*-alanine as an external reference (using the CH_3 signal at 20.5 ppm), corresponding to the same adamantane reference referred to above.

DFT GIPAW Calculations:

Calculations were performed by employing a plane-wave based DFT approach as implemented in the CASTEP code, UK academic release version 8.0 [40]. Initial atomic coordinates were taken from the published crystal structures [24] for which the ".cif" files are available on the Crystallography Open Database http://www.crystallography.net/cod/cod/4501669.html, with codes: 4501669 (293 K), 4501670 (235 K), 4501671 (150 K), 4501672 (100 K). All crystallographic parameters, such as cell dimensions and angles among others, are described in Ref [24]. The crystal structures obtained at 235 and 100 K both contain two ionic pairs per unit cell whilst those obtained at 150 and 293 K contain one. For the 235 and 293 K crystal structures, two different conformers are described, due to the disorder related to one of the ethyl groups. In these cases, two ".cif" files were created: for the first conformer the C7A', C8A', H8A1', H8A2', H8A3', H7A1' and H7A2' atoms were manually deleted; and for the second one these atoms

were preserved and the C7A, C8A, H8A1, H8A2, H8A3, H7A1 and H7A2 were instead manually deleted. Hence, a total of six ".cif" files were used for GIPAW calculations. (Note that calculated NMR parameters for the 293 K first conformer have been presented in Ref. [25].)

The unit cell parameters were fixed, space group symmetry was imposed, and periodic boundary conditions were applied during the geometry optimization. NMR shielding calculations were performed using the gauge-including projector-augmented wave (GIPAW) approach [41, 42]. Both geometry optimizations and NMR chemical shift calculations used a plane-wave basis set and the PBE exchange correlation functional [42, 43] at a basis cut-off energy of 700 eV, with integrals taken over the Brillouin zone by using a Monkhorst−Pack grid of minimum sample spacing $0.1 \times 2\pi$ Å^{-1}. A semi empirical dispersion correction was applied using the TS scheme [44] during both geometry optimization and NMR shielding calculations, employing ultrasoft pseudopotentials generated on the fly (OTF) [45]. After geometry optimization, the forces, energies and displacements were better than 0.05 eV Å^{-1}, 0.000002 eV and 0.0002 Å, respectively. Distances stated in this paper are for the geometry-optimised structures. GIPAW calculated NMR shielding were visualized, processed, and tabulated through the CCP-NC output files visualization tool, MagresView version 1.6 [46], running on Mozilla Firefox web browser version 49.0.2.

Results

^{1}H-^{13}C Heteronuclear Correlation 2D MAS NMR spectroscopy

Intermolecular interactions between $(DEC)^{+}$ and $(citrate)^{-}$ molecules are revealed by the ^{1}H-^{13}C CP-FSLG-HETCOR experiment. Two spectra were recorded with two different CP contact times: 50 (Fig. 1a) and 2000 μs (Fig. 1b). The experiment using 50 μs (Fig. 1a) exhibits mainly those cross peaks related to directly bonded carbon and hydrogen atoms. In Fig. 1b, the use of a longer CP contact time (2000 μs) leads to the observation of three correlations (shown by shaded circles) between the NH^{+} (H22) proton with carbons C8, C42 and C44. As shown on the right-hand side of Fig. 1, these correspond to close intramolecular (C8) and intermolecular (C42, C44) distances. Note that no correlation peaks with C9 and C7 are observed, with this likely being due to different spin dynamics for these CH_2 groups.

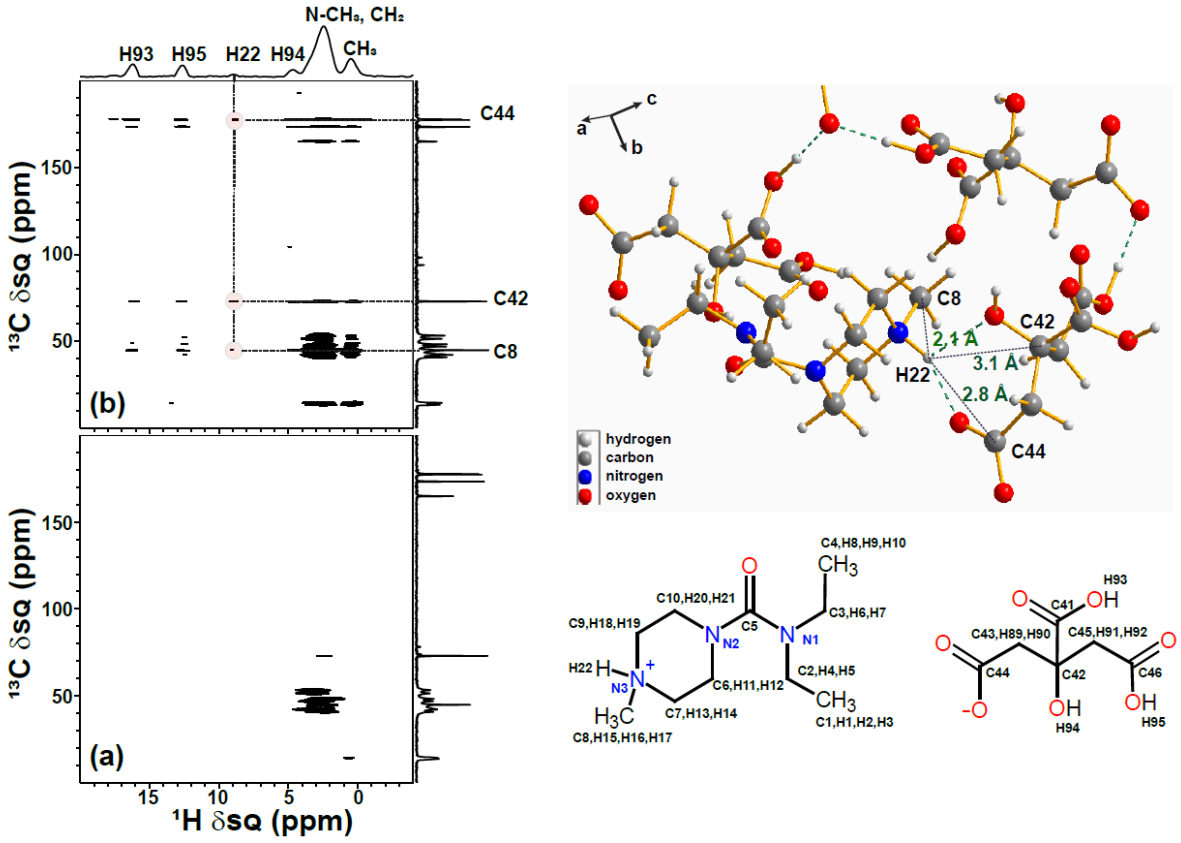

Figure 1: ^{1}H (500 MHz)-^{13}C HETCOR MAS NMR spectra of diethylcarbamazine citrate recorded using FSLG ^{1}H decoupling and CP contact times of (a) 50 (12.5 kHz) and (b) 2000 µs (10.0 kHz). The base contour is at (a) 20% and (b) 7% of the maximum height. The projections on the right-hand side of the two 2D spectra are ^{1}H-^{13}C CP MAS spectra recorded at the same magnetic field strength (11.4 T) using a 2 ms contact time. On the right hand side, a view of the geometry optimized (CASTEP) structure is shown; the proximities of H22 (NH^{+}) to C8, C42 and C44 corresponding to observed cross peaks (red highlighting in b) are indicated.

Variable-temperature ^{1}H-^{13}C CP MAS NMR spectroscopy

Figs. 2 and 3 present ^{1}H-^{13}C CP MAS spectra of the DEC-cit sample for two different temperatures ranges: below and above 0 ^{o}C, respectively. Consider first the spectra in Fig. 2 recorded at low temperatures: the chemical shifts for specific carbon atoms are observed to

increase upon increasing the temperature from –40 ºC to 0 ºC. The biggest changes are observed for carbons C1, C4 and C42.

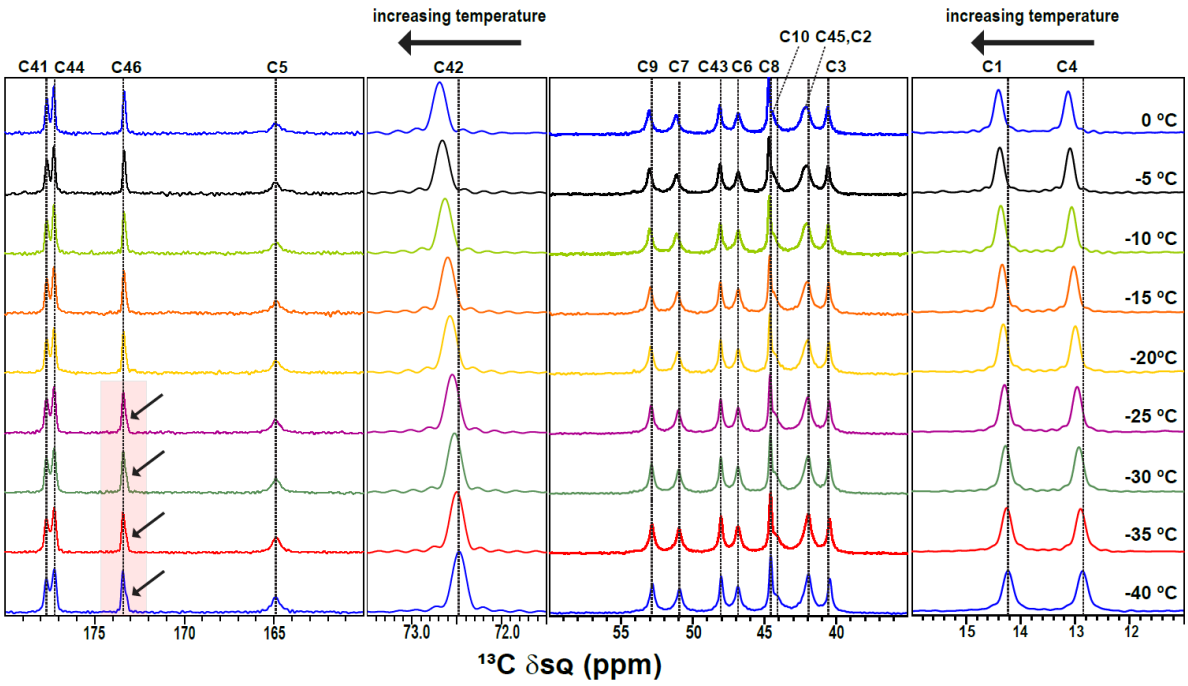

Figure 2: ^{1}H (500 MHz)-^{13}C CP MAS (5 kHz) spectra for diethylcarbamazine citrate at different temperatures from 0 to –40 ºC. Expanded regions are shown to improve the visualization.

Regarding the dynamics of the (citrate)$^{-}$ molecule, we can see evident changes for carbons C42 and C46. The chemical shift of C42 varies from 72.5 (–40 ºC) to 73.0 ppm (+50 ºC). It is also observed that the lineshape for carbon C46 changes for the lower temperature range (below –25 ºC), with a shoulder appearing (on the lower-ppm side) as highlighted by the arrows in Fig. 2. A closer look at this resonance is presented in Fig. 4. Specifically, it is possible to observe that the principal signal shifts to a higher ppm value as the temperature decreases, from 173.3 to 173.4 ppm, while below –25 ºC a slight shoulder starts to appear at 173.2 ppm (see the red shaded area in Fig. 2).

Consider now changes for the (DEC)$^{+}$ unit. Further to changes for C1 and C4 (assigned to the terminal CH_3 groups of the ethyl moieties) observed at low temperature (Fig. 2), the most interesting changes take place at higher temperatures (above 20 ºC, see Fig. 3). Specifically, a

broadening of the C1 and C4 resonances is observed, followed by coalescence at 35 °C, before the resonances start to narrow at around 14 ppm at 40 °C and higher temperatures. This corresponds to the well-known exchange phenomenon on moving from slow exchange to intermediate exchange to fast exchange. [47-50]. Marked temperature-dependent changes are also observed for the peaks between 40 and 45 ppm, notably at 42.5 and 44.5 ppm with considerable broadening at some temperatures. This is a crowded region of the spectrum corresponding to C2, C3, C8, C10 and C45, with the obvious explanation being that the changes are for C2 and C3. Only small changes (see C7 and C9 in Fig. 3) are observed for the carbons from the piperazine 6-member ring, showing that the chair conformation of this ring is preserved.

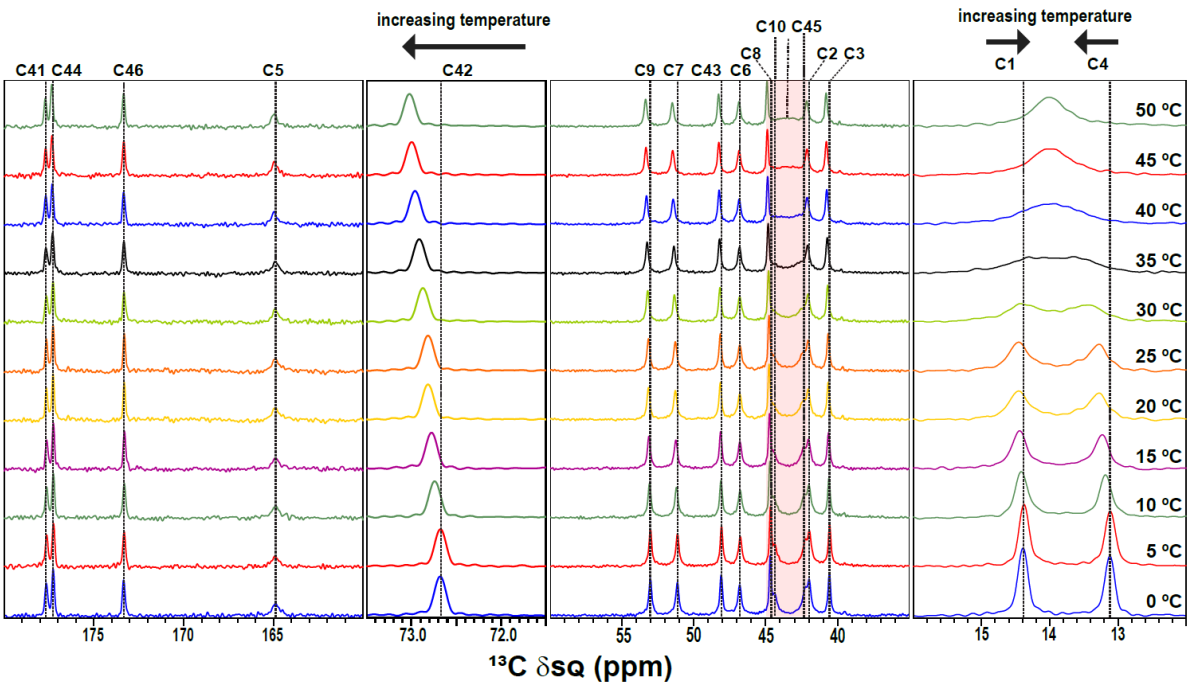

Figure 3: ^{1}H (500 MHz)-^{13}C CP MAS (5 kHz) spectra for diethylcarbamazine citrate at different temperatures from 0 to +50 °C. Expanded regions are shown to improve the visualization.

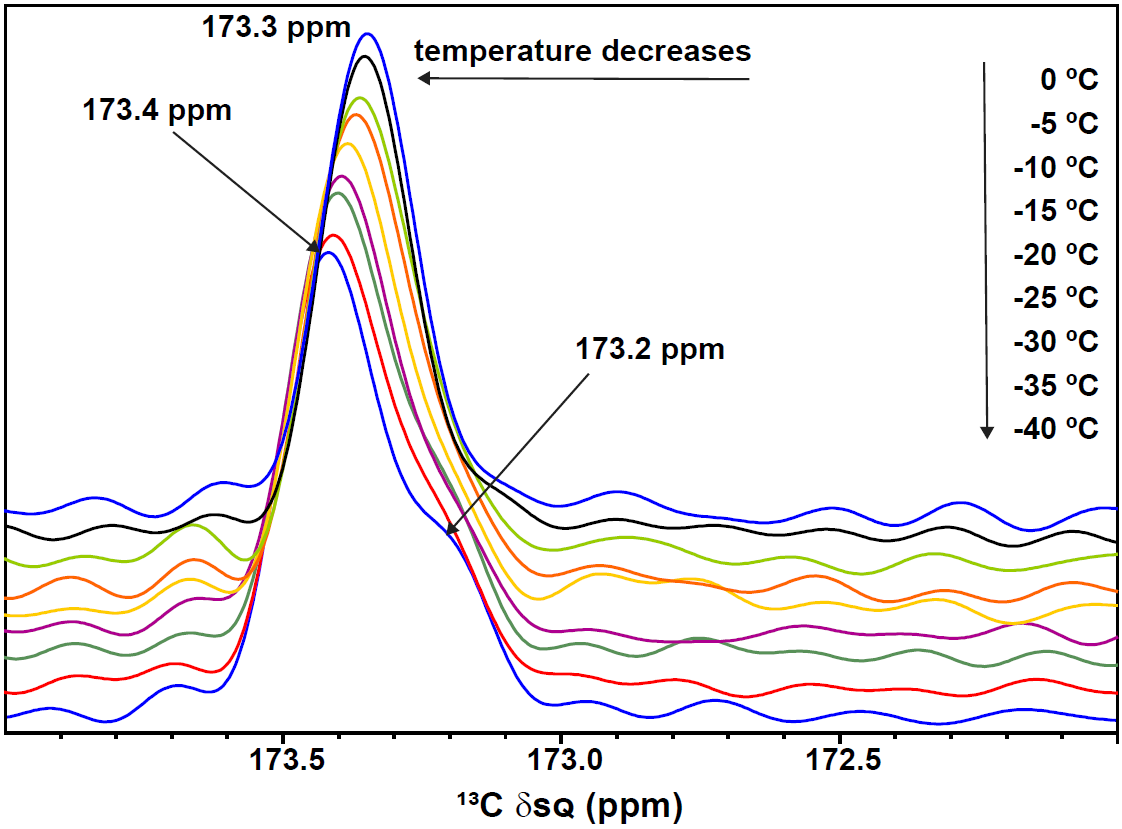

Figure 4: ^{1}H (500 MHz)-^{13}C CP MAS (5 kHz) spectra for diethylcarbamazine citrate at different temperatures from 0 to –40 °C. Expanded regions are shown so as to better visualize changes for the C46 resonance.

Using GIPAW calculations to interpret the experimental MAS NMR observations

When Silva et al [24] described the room-temperature crystal structure of DEC citrate salt, they also reported the existence of three phase transitions between four different phases at 293, 235, 150 and 100 K, mostly involving changes for the two ethyl moieties (i.e, C1, C2, C3, C4). For the 235 and 293 K structures, they also describe the existence of two possible conformers, related to the observed disorder. Table 1 lists the GIPAW calculated chemical shifts for these distinct crystal structures and conformers (after initial geometry optimisation). The Table also lists the maximum range for each chemical site, with the biggest changes (> 3 ppm) for ^{13}C observed for C1 to C6 and C45.

Table 1: Experimental[a] (293K) and GIPAW[b] calculated isotropic NMR chemical shifts (in ppm) for different phases of the diethycarbamazine citrate salt at different temperatures (100, 150, 235 and 293 K).

Atom	XRD labelling [24]	Atom descriptor	phase 100K		phase 150 K	phase 235 K				phase 293 K		$\Delta\delta_{iso}^{calc}$ (max over all phases)	Experimental 293 K
						conformer 1		conformer 2		conformer 1	conformer 2		
			molecule 1	molecule 2		molecule 1	molecule 2	molecule 1	molecule 2	Ref [25]			Ref [25]
			δ_{iso}^{calc}	δ_{iso}^{calc}	δ_{iso}^{calc}	δ_{iso}^{calc}	δ_{iso}^{calc}	δ_{iso}^{calc}	δ_{iso}^{calc}	δ_{iso}^{calc}	δ_{iso}^{calc}		δ_{iso}^{exp}
C1	**C10A**	**CH_3**	14.1	10.5	10.4	10.6	10.4	13.2	10.5	10.9	13.7	3.7	14.2
C2	**C9A**	**CH_2**	45.3	41.0	41.0	42.1	41.1	50.9	41.2	42.0	44.3	9.9	42.1
C3	**C7A**	**CH_2**	47.8	41.2	41.2	40.0	41.1	44.9	41.2	40.5	50.6	10.6	40.7
C4	**C8A**	**CH_3**	9.9	8.6	8.7	8.6	8.7	14.2	8.8	8.6	13.0	5.6	13.6
C5	**C6A**	**C=O**	161.4	162.6	158.5	163.3	158.8	160.6	158.7	163.0	160.1	4.6	164.9
C6	**C4A**	**CH_2**	47.0	48.7	46.5	49.0	46.8	49.6	46.7	49.3	46.5	3.1	48.2
C7	**C3A**	**CH_2**	51.3	50.4	51.5	50.8	51.7	50.3	51.5	50.9	50.6	1.4	51.3
C8	**C5A**	**CH_3**	44.7	44.7	44.4	44.0	44.3	44.9	44.3	44.2	44.5	0.9	44.8
C9	**C2A**	**CH_2**	53.0	52.7	53.3	53.3	53.4	53.0	53.2	53.0	52.9	0.7	53.2
C10	**C1A**	**CH_2**	40.9	43.9	42.2	43.1	42.6	42.3	41.6	43.4	41.9	3.0	44.5
C41	**C6C**	**COOH**	181.4	181.8	180.8	181.0	180.9	180.7	181.0	180.9	180.7	1.1	177.6
C42	**C3C**	**Cq**	74.2	74.3	74.0	74.5	73.8	74.0	73.7	74.2	73.7	0.8	72.8
C43	**C2C**	**CH_2**	49.7	49.9	49.2	49.6	49.0	49.0	49.3	49.1	48.7	1.2	46.8
C44	**C1C**	**COO^-**	179.9	179.7	179.3	179.3	179.6	179.0	179.4	179.3	179.0	0.9	177.3
C45	**C4C**	**CH_2**	53.6	41.7	42.9	42.5	53.8	42.3	42.6	42.6	41.7	12.1	42.4
C46	**C5C**	**COOH**	176.7	176.6	176.6	176.1	176.9	176.3	176.9	176.3	176.1	0.8	173.3
H1,H2,H3	**H10A1,H10A2,H10A3**	**CH_3**	0.2	0.4	0.1	0.4	0.2	0.5	0.2	0.4	0.4	0.4	0.5
H4	**H9A1**	**CH_2**	2.8	2.5	2.4	2.6	2.5	2.3	2.5	2.5	2.2	0.6	2.5
H5	**H9A2**	**CH_2**	2.4	2.5	2.4	2.4	2.5	2.8	2.5	2.3	2.7	0.5	2.5
H6	**H7A1**	**CH_2**	2.9	2.6	2.7	2.6	2.9	2.8	2.9	2.1	1.9	1.0	2.3

H7	**H7A2**	**CH_2**	2.1	2.1	2.2	2.2	2.3	2.0	2.3	2.5	2.8	0.8	2.3
H8, H9,H10	**H8A1, H8A2, H8A3**	**CH_3**	0.3	0.2	0.2	0.2	0.3	0.0	0.3	0.1	-0.1	0.4	0.5
H11	**H4A1**	**CH_2**	2.7	2.7	2.8	2.8	3.0	2.8	3.0	2.7	2.7	0.3	2.7
H12	**H4A2**	**CH_2**	2.8	2.8	3.0	2.9	3.1	2.9	3.1	2.8	2.8	0.3	2.7
H13	**H3A1**	**CH_2**	2.7	3.1	2.6	3.1	2.6	3.2	2.6	2.9	3.0	0.5	2.8
H14	**H3A2**	**CH_2**	3.1	3.2	3.0	3.2	3.1	3.4	3.1	3.3	3.4	0.4	2.8
H15,H16,H17	**H5A1, H5A2, H5A3**	**CH_3**	2.2	2.1	2.2	2.3	2.3	2.3	2.3	2.1	3.1	1.0	2.3
H18	**H2A1**	**CH_2**	2.4	2.4	2.4	2.4	2.6	2.4	2.6	2.4	2.3	0.3	2.7
H19	**H2A2**	**CH_2**	3.1	3.0	3.0	3.1	3.0	3.1	3.0	3.0	3.0	0.1	2.7
H20	**H1A1**	**CH_2**	3.7	3.6	3.8	3.7	3.9	3.7	3.9	3.6	3.7	0.3	2.9
H21	**H1A2**	**CH_2**	2.7	2.5	2.6	2.9	2.6	2.9	2.7	2.7	2.8	0.4	2.9
H22	**H2A**	**N^+H**	9.2	9.2	8.7	9.7	8.7	9.4	8.7	9.4	9.2	1.0	9.1
H89	**H2C1**	**CH_2**	1.5	1.7	1.4	1.7	1.5	1.7	1.5	1.6	1.6	0.3	2.5
H90	**H2C1**	**CH_2**	2.3	2.3	2.1	2.4	2.2	2.3	2.3	2.3	2.3	0.3	2.5
H91	**H4C1**	**CH_2**	2.6	2.5	2.4	2.5	2.6	2.5	2.6	2.5	2.4	0.2	2.7
H92	**H4C2**	**CH_2**	2.1	2.2	2.1	2.3	2.2	2.3	2.2	2.1	2.1	0.2	2.7
H93	**H6C**	**COOH**	17.1	17.1	17.4	16.9	17.5	16.9	17.3	16.7	16.9	0.8	16.2
H94	**H3C**	**OH**	4.4	4.5	4.2	4.4	4.2	3.8	4.3	4.2	3.6	0.9	4.8
H95	**H7C**	**COOH**	14.1	14.0	13.9	14.1	14.2	14.1	14.2	14.3	14.2	0.4	12.8
N1	**N2A**	**N(C=O)N**	-284.1	-282.1	-275.6	-285.7	-275.0	-274.3	-274.9	-286.8	-274.9	12.5	-287.7
N2	**N1A**	**N(C=O)N**	-296.4	-300.0	-304.6	-299.2	-305.1	-308.6	-305.2	-309.4	-309.1	13.0	-308.4
N3	**N3A**	**N^+H**	-331.0	-330.6	-331.0	-331.3	-330.4	-331.8	-330.6	-328.6	-331.4	3.2	-336.4

[a] It is not possible to distinguish and separate CH_2 and CH_3 ^1H resonances in the experimental spectra.

[b] Calculated isotropic chemical shifts are given by $\delta_{iso}^{calc} = \sigma_{ref} - \sigma_{calc}$, where σ_{ref} was 30 ppm for ^{1}H and −153 ppm for $^{14}N/^{15}N$. For ^{13}C, two shielding references were determined: σ_{ref} = 170 ppm for $\delta_{iso} \geq 70$ ppm and σ_{ref} = 173 ppm for $\delta_{iso} \leq 70$ ppm [51]. For CH_3 groups, the stated calculated isotropic chemical shift corresponds to the average for the three protons.

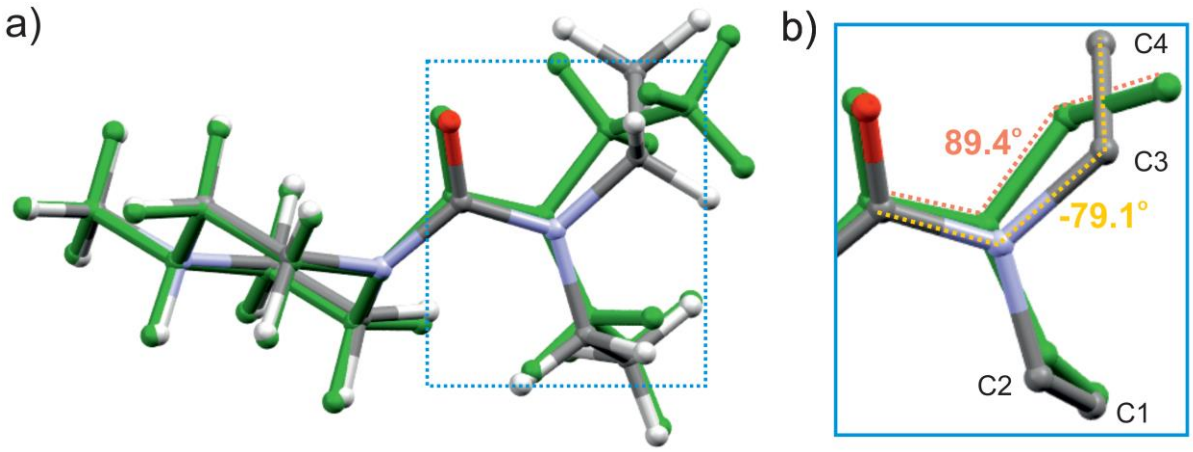

Figure 5: Geometry optimized structures of both conformers (from the X-ray diffraction structure) of diethylcarbamazine at 293 K (conformer 2 is shown in green): (a) the full $(DEC)^+$ molecule, (b) a zoomed-in view for the carbon atoms that exhibit disorder, with the dihedral angles noted.

It is clearly observed that the carbons C1 to C5 are involved in the disorder and their chemical shifts follows the changes in their orientation, as revealed by GIPAW calculations at 293 K. According to these calculations, C3 and C4 are mostly affected, and this finding reflects the differences in their chemical shifts ($\Delta\delta$ is 10.1 and 4.4 ppm, respectively), as well as the dihedral angles (see Fig. 5). By comparison, for C1, C2 and C5, $\Delta\delta$ is 2.8, 2.3 and 2.9 ppm, respectively. Indeed, Silva *et al* [24] have already described a non-classical intermolecular hydrogen bond formed between the terminal CH_3 (C1) group from the DEC unit with a carboxyl group from a citrate unit. They report that this interaction is responsible for keeping this methyl group ordered, in contrast to the second one (C4). Surprisingly small changes are observed in Table 1 for protons bonded to C1-C4. A $\Delta\delta$ of 11.9 is observed for the calculated ^{15}N chemical shift of nitrogen N1, also involved in the disorder.

When we compare the calculated chemical shifts with the experimental ones, an interesting behaviour is observed. The experimental chemical shifts of C1 and C4 have a good agreement with the calculated ones for conformer 2. However, the experimental chemical shifts for C2, C3 and C5 exhibit a better agreement with those calculated for conformer 1. In the supporting information full spectra are shown in Fig. S1, and no signals can be observed below 10 ppm, except for spinning sideband peaks. To explore this interesting finding, we prepared ".cif" files for two new conformers, named conformer 3 and 4. For conformer 3, we

took the ".cif" file from conformer 1, replacing the atomic coordinates of C1 and C4 by those ones from conformer 2. The ".cif" file for conformer 4 was prepared from the atomic coordinates of conformer 2, replacing the positions of C1 and C4 by those from conformer 1. These new structures were optimized using DFT (in CASTEP), and the chemical shifts were calculated by using the GIPAW method – see Table 2. Additionally, the optimized $(DEC)^+$ structures are shown in Fig. 6.

Table 2. Experimental (293K) [25] and GIPAW[a] calculated isotropic NMR chemical shifts for ^{13}C nuclei for different conformers of the diethycarbamazine citrate salt[a] at 293 K.

C[b]		**δ_{iso} calc / ppm**	**δ_{iso} calc ppm**	**δ_{iso} calc / ppm**	**δ_{iso} calc / ppm**	**δ_{iso} exp**
		conformer 1[c]	conformer 2[c]	conformer 3[d]	conformer 4[e]	ppm
C1	***CH_3***	*10.9*	*13.7*	*13.8*	*9.6*	*14.2*
C2	***CH_2***	*42.0*	*44.3*	*50.0*	*42.6*	*42.1*
C3	***CH_2***	*40.5*	*50.6*	*45.9*	*41.5*	*40.7*
C4	***CH_3***	*8.6*	*13.0*	*13.5*	*8.0*	*13.6*
C5	***C=O***	*163.0*	*160.1*	*160.5*	*163.4*	*164.9*
C6	**CH_2**	49.3	46.5	46.6	48.8	48.2
C7	**CH_2**	50.9	50.6	50.8	50.1	51.3
C8	**CH_3**	44.2	44.5	44.3	44.1	44.8
C9	**CH_2**	53.0	52.9	53.6	52.7	53.2
C10	**CH_2**	43.4	41.9	42.7	43.2	44.5
C41	**COOH**	180.9	180.7	180.3	180.9	177.6
C42	**Cq**	74.2	73.7	74.2	75.2	72.8
C43	**CH_2**	49.1	48.7	48.9	48.8	46.8
C44	**COO^-**	179.3	179.0	178.8	178.7	177.3
C45	**CH_2**	42.6	41.7	42.1	41.9	42.4
C46	**COOH**	176.3	176.1	176.6	175.1	173.3

[a] Calculated isotropic chemical shifts are given by $\delta_{iso}^{calc} = \sigma_{ref} - \sigma_{calc}$, where two shielding references were determined: σ_{ref} = 170 ppm for $\delta_{iso} \geq 70$ ppm and σ_{ref} = 173 ppm for $\delta_{iso} \leq 70$ ppm [51], as presented in Table 1.

[b] Italic denotes the carbons affected most by changing the positions of C1 and C4.

[c] optimized from the original ".cif" file, conformer 1 values taken from Ref. [25].

[d] prepared from the ".cif" file of conformer 1, replacing the C1 and C4 atomic coordinates by those ones from conformer 2.

[e] prepared from the ".cif" file of conformer 2, replacing the C1 and C4 atomic coordinates by those ones from conformer 1.

Upon a second comparison between the experimental MAS NMR data with the full set of calculated data in Table 2, we conclude that our experimental solid-state NMR data is most similar to the conformer 1, with the prevision that the C1 and C4 of the methyl groups are more affected by dynamics, as revealed by the variable temperature ^{13}C CP MAS NMR spectra in Figs. 2 and 3.

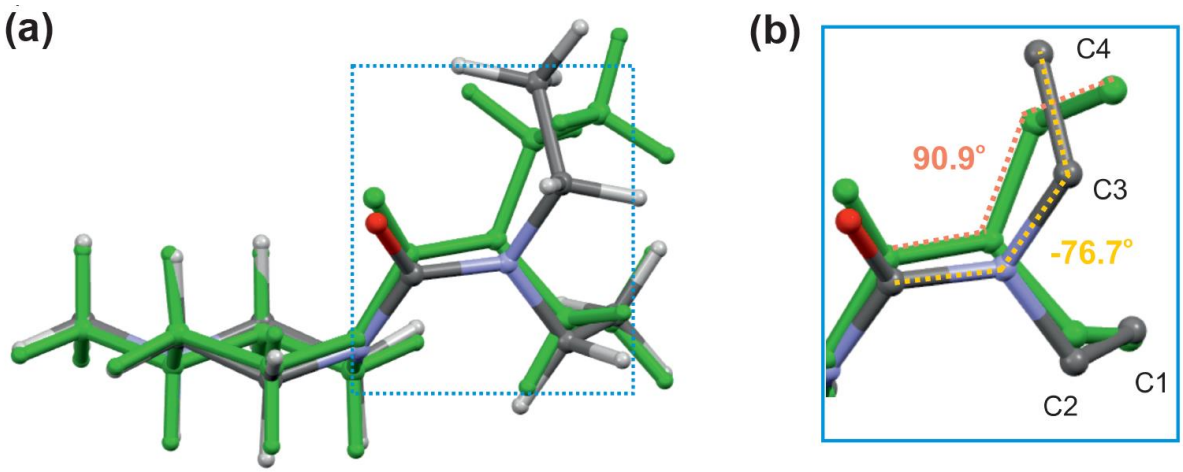

Figure 6: Geometry optimized structures of as-constructed (see discussion in the main text) conformers 3 and 4 of diethylcarbamazine at 293 K (conformer 4 is shown in green): (a) the full $(DEC)^+$ molecule, (b) a zoomed-in view for the carbon atoms that exhibit disorder, with the dihedral angles noted.

As shown in Figures 2 to 4, some slow dynamics is observed for the $(citrate)^-$ molecule. However, it is curious that no evident temperature-dependent experimental changes are observed for most of the ^{13}C chemical shifts of $(citrate)^-$ molecule, except for C42 and C46 (as discussed above). Table 1 shows that the GIPAW calculated ^{13}C chemical shifts for C42 are different for the two conformers at 293K (73.7 and 74.2 ppm) such that a change in relative population for the two distinct conformers could be an explanation for the experimental findings.

For carbon C46, a shift from 176.3 ppm (at 293 K) to an average chemical shift of 176.9 ppm (235 K) is observed, if only the most probable conformer (conformer 1) is considered. However, the XRD analysis also predicts the existence of two molecules in the same unit cell for this conformer [24] and the GIPAW calculations indicate two values of 176.9 and 176.1

ppm for the C46 resonance. Similarly, two distinct values of 176.9 and 176.1 ppm are also calculated for the other conformer (conformer 2). Since the changes in both the calculated and experimental ^{13}C chemical shifts are small, it is not possible to offer a clear explanation, but the appearance of the shoulder at 173.2 ppm at low temperature (see red shading in Fig. 2) may be an indication of the start of the phase transition whereby two distinct resonances are observed due to the two distinct molecules in the asymmetric unit cell for the 235 K phase.

Conclusions

Variable temperature ^{13}C solid state NMR spectra provide insight into the dynamics of both DEC and citrate molecules. The chair conformation of piperazine 6-member ring from DEC molecule does not change, with no significant chemical shift changes being observed. In contrast, ethyl moieties exhibit the biggest variation, in line with disorder in the XRD structures. Additionally, some dynamics was observed for the citrate unit, not described by XRD data. GIPAW calculations are particularly useful to explain changes observed in the experimental spectra, as well as to explore the possibility of having four different conformers for $(DEC)^{+}(citrate)^{-}$ salt, indicating that there is a major conformer. The challenge for describing a precise crystal structure for this salt is the high mobility of methyl groups (C1 and C4) of the DEC molecule, as observed by variable temperature ^{13}C CP MAS NMR.
In contrast to XRD methods, solid state NMR provided insights on the fast exchange dynamics showing the conformational changes involving particularly the ethyl moieties of diethylcarbamazine molecule. GIPAW calculations were especially useful to monitor the carbons involved in disorder, previously described, and allowed the possibility of having an average structure between two conformers at 293 K to be explored. Particularly for GIPAW calculations, it is still challenging to include the effect of temperature, but initial results are being presented [19, 30, 52, 53]. A recent approach uses the combination of molecular dynamics and path integer approach to treat the system in terms of quantum mechanics [54-56], but it is still computationally expensive and not fully available in routine jobs.

Acknowledgements

We would like to acknowledge Fundação Osvaldo Cruz – Instituto de Tecnologia de Fármacos -Farmanguinhos for providing the sample used in this work. CASTEP calculations were performed at the University of Warwick Centre for Scientific Computing. T. V. thanks the Fundação de Amparo à Pesquisa do Estado de São Paulo (FAPESP, processes: 2009/13860-2 and 2015/21708-7) and INCP-CBIP/UFSCar, while L.M.A.M. thanks CNPq (process: 142384/2010-0). Tomasz Pawlak thanks the Polish Ministry of Science and Higher Education for support ("Mobility Plus" program, no. 1318/MOB/IV/2015/0). The calculated and experimental data for this study are provided as a supporting dataset from WRAP, the Warwick Research Archive Portal at http://wrap.warwick.ac.uk/***.

References

[1] A. E. Gray, G. M. Day, M. Leslie,S. L. Price, *Mol. Phys.* **2004**, *102*, 1067.
[2] C. Ouvrard,S. L. Price, *Cryst. Growth Des.* **2004**, *4*, 1119.
[3] S. L. Price, *Adv. Drug Deliver. Rev.* **2004**, *56*, 301.
[4] R. M. Bhardwaj, L. S. Price, S. L. Price, S. M. Reutzel-Edens, G. J. Miller, I. D. H. Oswald, B. F. Johnston,A. J. Florence, *Cryst. Growth Des.* **2013**, *13*, 1602.
[5] S. L. Price, *Chem. Soc. Rev.* **2014**, *43*, 2098.
[6] S. L. Price, *CrystEngComm* **2004**, *6*, 344.
[7] S. L. Price, D. E. Braun,S. M. Reutzel-Edens, *Chem. Commun.* **2016**, *52*, 7065.
[8] S. L. Price,S. M. Reutzel-Edens, *Drug Discov. Today* **2016**, *21*, 912.
[9] M. Tremayne, L. Grice, J. C. Pyatt, C. C. Seaton, B. M. Kariuki, H. H. Y. Tsui, S. L. Price,J. C. Cherryman, *J. Am. Chem. Soc.* **2004**, *126*, 7071.
[10] O. G. Uzoh, A. J. Cruz-Cabeza,S. L. Price, *Cryst. Growth Des.* **2012**, *12*, 4230.
[11] J. R. Reimers, D. Panduwinata, J. Visser, Y. Chin, C. G. Tang, L. Goerigk, M. J. Ford, M. Sintic, T. J. Sum, M. J. J. Coenen, B. L. M. Hendriksen, J. Elemans, N. S. Hush,M. J. Crossley, *P. Natl. Acad. SciI. USA* **2015**, *112*, E6101.
[12] D. C. Apperley, A. F. Markwell, I. Frantsuzov, A. J. Ilott, R. K. Harris,P. Hodgkinson, *Phys. Chem. Chem. Phys.* **2013**, *15*, 6422.
[13] K. M. Hutchins, R. H. Groeneman, E. W. Reinheimer, D. C. Swenson,L. R. MacGillivray, *Chem. Sci.* **2015**, *6*, 4717.
[14] T. Polenova, R. Gupta,A. Goldbourt, *Anal. Chem.* **2015**, *87*, 5458.
[15] X. Zhang, X. D. Shao, S. C. Li, Y. Cai, Y. F. Yao, R. G. Xiong,W. Zhang, *Chem. Commun.* **2015**, *51*, 4568.
[16] J. Ellena, K. de Paula, C. C. de Melo, C. C. P. da Silva, B. P. Bezerra, T. Venancio,A. P. Ayala, *Cryst. Growth Des.* **2014**, *14*, 5700.
[17] E. Shalaev, K. Wu, S. Shamblin, J. F. Krzyzaniak,M. Descamps, *Adv. Drug Deliver. Rev.* **2016**, *100*, 194.
[18] M. Dracinsky,P. Hodgkinson, *CrystEngComm* **2013**, *15*, 8705.
[19] X. Z. Li, L. Tapmeyer, M. Bolte,J. van de Streek, *Chemphyschem* **2016**, *17*, 2496.
[20] A. Davis,D. R. Bailey, *Bull. World Health Organ.* **1969**, *41*, 195.
[21] E. Kimura,J. U. Mataika, *Parasitol. Today* **1996**, *12*, 240.

[22] A. Weaver, P. Brown, S. Huey, M. Magallon, E. B. Bollman, D. Mares, T. G. Streit,M. Lieberman, *PLoS Negl.Trop. Dis.* **2011**, *5*, e1005.
[23] S. B. Honorato, C. C. P. da Silva, Y. S. de Oliveira, J. S. Mendonca, N. Boechat, J. Ellena,A. P. Ayala, *J. Pharm. Sci.* **2016**, *105*, 2437.
[24] C. C. P. da Silva, F. T. Martins, S. B. Honorato, N. Boechat, A. P. Ayala,J. Ellena, *Cryst. Growth Des.* **2010**, *10*, 3094.
[25] T. Venancio, L. M. Oliveira, J. Ellena, N. Boechat,S. P. Brown, *Solid State Nucl. Magn. Reson.* **2017**, *87*, 73.
[26] P. Schanda,M. Ernst, *Prog. Nucl. Magn. Reson. Spectrosc.* **2016**, *96*, 1.
[27] A. Paudel, M. Geppi,G. Van den Mooter, *J. Pharm. Sci.* **2014**, *103*, 2635.
[28] N. E. De Almeida, K. J. Harris, A. Samoson,G. R. Goward, *J. Phys. Chem. C* **2016**, *120*, 19961.
[29] P. Guerry, S. P. Brown,M. E. Smith, *Aip Advances* **2016**, *6*, 055008.
[30] S. E. Ashbrook,D. McKay, *Chem. Commun.* **2016**, *52*, 7186.
[31] A. E. Bennett, C. M. Rienstra, M. Auger, K. V. Lakshmi,R. G. Griffin, *J. Chem. Phys.* **1995**, *103*, 6951.
[32] I. Scholz, P. Hodgkinson, B. H. Meier,M. Ernst, *J. Chem. Phys.* **2009**, *130*, 114510.
[33] G. Metz, X. L. Wu,S. O. Smith, *J. Magn. Reson., Ser. A* **1994**, *110*, 219.
[34] C. R. Morcombe,K. W. Zilm, *J. Magn. Reson.* **2003**, *162*, 479.
[35] S. Hayashi,K. Hayamizu, *Bull. Chem. Soc. Jpn.* **1991**, *64*, 685.
[36] B. J. van Rossum, H. Forster,H. J. M. de Groot, *J. Magn. Reson.* **1997**, *124*, 516.
[37] A. Bielecki, A. C. Kolbert,M. H. Levitt, *Chem. Phys. Lett.* **1989**, *155*, 341.
[38] M. H. Levitt, A. C. Kolbert, A. Bielecki,D. J. Ruben, *Solid State Nucl. Magn. Reson.* **1993**, *2*, 151.
[39] B. M. Fung, A. K. Khitrin,K. Ermolaev, *J. Magn. Reson.* **2000**, *142*, 97.
[40] S. J. Clark, M. D. Segall, C. J. Pickard, P. J. Hasnip, M. J. Probert, K. Refson,M. C. Payne, *Z. Kristallogr.* **2005**, *220*, 567.
[41] C. J. Pickard,F. Mauri, *Phys. Rev. B: Condens. Matter* **2001**, *63*, 245101.
[42] J. R. Yates, C. J. Pickard,F. Mauri, *Phys. Rev. B: Condens. Matter* **2007**, *76*, 024401.
[43] J. P. Perdew, K. Burke,M. Ernzerhof, *Phys. Rev. Lett.* **1996**, *77*, 3865.
[44] A. Tkatchenko,M. Scheffler, *Phys. Rev. Lett.* **2009**, *102*, 073005.
[45] D. Vanderbilt, *Phys. Rev. B: Condens. Matter* **1990**, *41*, 7892.
[46] S. Sturniolo, T. F. G. Green, R. M. Hanson, M. Zilka, K. Refson, P. Hodgkinson, S. P. Brown,J. R. Yates, *Solid State Nucl. Magn. Reson.* **2016**, *78*, 64.
[47] S. P. Brown, T. Schaller, U. P. Seelbach, F. Koziol, C. Ochsenfeld, F. G. Klarner,H. W. Spiess, *Angew. Chem. Int. Ed.* **2001**, *40*, 717.
[48] J. M. Twyman,C. M. Dobson, *J. Chem. Soc. Chem. Comm.* **1988**, 786.
[49] R. K. Harris, *Analyst* **2006**, *131*, 351.
[50] A. Abraham, D. C. Apperley, S. J. Byard, A. J. Ilott, A. J. Robbins, V. Zorin, R. K. Harris,P. Hodgkinson, *CrystEngComm* **2016**, *18*, 1054.
[51] A. L. Webber, L. Emsley, R. M. Claramunt,S. P. Brown, *J. Phys. Chem. A* **2010**, *114*, 10435.
[52] B. Monserrat, R. J. Needs,C. J. Pickard, *J. Chem. Phys.* **2014**, *141*,
[53] R. Nemausat, D. Cabaret, C. Gervais, C. Brouder, N. Trcera, A. Bordage, I. Errea,F. Mauri, *Phys. Rev. B: Condens. Matter* **2015**, *92*,
[54] A. Jezierska,J. J. Panek, *Journal of Computational Chemistry* **2009**, *30*, 1241.
[55] P. Durlak,Z. Latajka, *Phys. Chem. Chem. Phys.* **2014**, *16*, 23026.
[56] M. Dracinsky, L. Cechova, P. Hodgkinson, E. Prochazkova,Z. Janeba, *Chem. Commun.* **2015**, *51*, 13986.